Supporting Information

Whole house emission rates and loss coefficients of formaldehyde and other VOCs as a function of air change rate

Yibo Huangfu[1], Nathan M. Lima[1,2], Patrick T. O'Keeffe[1], William M. Kirk[2], Brian K. Lamb[1], Von P. Walden[1], Bertram T. Jobson[1*]

[1] Laboratory for Atmospheric Research, Department of Civil and Environmental Engineering, Washington State University, Pullman, WA, USA

[2] School of Architecture and Construction Management, Washington State University, Pullman, WA, USA

* Corresponding author

Number of Pages = 19

Number of Figures = 9

Number of Tables = 2

HVAC / HRV Systems

The home's ventilation system is designed to be a balanced system. The home has a conventional HVAC system using a Goodman AEPF air handler and a Goodman SS-Z14 high efficiency heat pump. The cooling coil for air-conditioning in summer was set to 40 °F. In a somewhat atypical configuration, the HRV system is separate from the HVAC system with its own separate ducting. The HRV is a Goodman HRV-300D with fans for both return and supply flows. The house is constructed monolithically using insulated concrete forms (ICF) with walls poured from the basement footing to the height of the first-floor ceiling framing. With all of the HVAC and HRV supply and return air ducts located either in the first floor cavity or in interior walls, the goal of the design is to eliminate air loss to the outside of the building envelope. The HVAC has two primary return grills: 1) upstairs entrance hallway 2) downstairs on a wall near the furnace room, and two smaller secondary grills: 3) upstairs master bedroom 4) upstairs guest bedroom bathroom. There are four return vents for the HRV: 1) the upstairs master bedroom; 2) master bathroom; 3) downstairs basement ceiling vent in the open area "game room"; 4) downstairs bathroom. There are two HRV supply vents. One is located in the downstairs as a ceiling vent and two are upstairs in the kitchen as floor level vents. The homeowner can operate the HRV using a push button control whereby the HRV will turn on at the high air flow rate (180 CFM) for 20 minutes.

Instrumentation

The instrumentation consisted of monitors for O_3, CO, and NO_x (Teledyne Inc.), CO_2 and H_2O (LiCor 840A), CH_4 (Los Gatos UGGA), $PM_{2.5}$ (TSI DustTrak II) and a quadrupole PTR-MS (Ionicon Analytik) to measure selected VOCs. For gases, an outdoor inlet consisting of 3/8"

OD PFA tubing ran from the instrumented room out a window opening to a tripod mounted on the roof of the house. The window opening was then sealed to prevent additional air exchange. The indoor air inlet was ½" OD PFA tubing that ran from the instruments in the room along the ceiling to the living room area. Air was continuously pulled through the indoor and outdoor inlets by external diaphragm pumps at 20 L min^{-1}, and the instrumentation subsampled these flows alternating every 15 minutes between indoor and outdoor air sampling. For PM sampling two different monitors were used without sampling inlets; one was placed in the living room and the other located outside. The 10-m meteorological tower erected in the backyard ~ 30-m from the house supported an Airmar WX200 weather station.

The PTR-MS drift tube was operated at 120 Td (60 °C drift tube temperature and 2 mbar drift tube pressure), with O_2^+/H_3O^+ ratio less than 2% and NO^+/H_3O^+ ratio less than 0.2%. The PTR-MS was calibrated with diluted multi-component compressed gas standards (Scott Marrin, CA and Apel-Reimer Environmental, FL; ± 5% accuracy). Monoterpene response was calibrated using α-pinene. For *m/z* 47, attributed to ethanol and formic acid, we assumed the response factor for formic acid. The PTR-MS response to ethanol was about a factor of ten lower than that of formic acid. In this house alcoholic beverages were not consumed but event emissions at this mass were observed and attributed to ethanol from consumer products or cooking. Peak concentrations of *m/z* 47 are thus likely greater that displayed in Figure S-3. For the compounds that were not included in the gas standards (acetic acid, formic acid, hexanoic acid, furfural, and acrylonitrile) response factors were calculated using the response factor for a compound with a similar mass from the compressed gas standard (to account for ion transmission efficiency) multiplied by the ratio of their respective H_3O^+ rate coefficients (to account for differences in reactivity). Thermal rate coefficients at the drift tube temperature

were calculated according to Su and Chesnavich [2] and Su [3]. For hexanoic acid and furfural, relevant parameters for calculating the rate constant could not be found and a rate constant of 2.5 x 10^{-9} cm^3 $molecule^{-1}$ s^{-1} was assumed.

We have been using the PTR-MS to measure formaldehyde for a number of years and have documented basic issues with water vapor sensitivity in Jobson and McCoskey [3], and noted elsewhere [4,5,6]. The formaldehyde response factors are a non-linear function of water vapor concentration and are dependent on drift operating conditions. Instrument response to formaldehyde was determined as a function of water vapor concentration using a formaldehyde permeation source (KinTek, TX, USA, with an accuracy of 2%). The water cluster ion isotope (*m/z* 39) was used as a tracer of water vapor concentration to account for changes in formaldehyde response factors during field measurements, where accounting for response factor differences between indoor and outdoor sampling was the primary issue. We are aware of a number of interferences for formaldehyde measurements by PTR-MS, notably a positive interference from fragmentation of CH_3OOH (methylhydroperoxide) which is not a significant issue indoors due to low concentrations of CH_3OOH in ambient air and high concentrations of formaldehyde indoors. A potentially more important positive interference is from O_2^+ reactions with methanol and ethanol [7-10]. When these alcohols are very elevated, which can happen indoors as a result of consumer product use, alcohol use, and cooking, a significant *m/z* 31 signal can result. We have determined relevant corrections factors for the drift tube conditions in this study from laboratory tests by preparing test gas mixtures of methanol and ethanol and determining *m/z* 31 yields as a function of O_2^+ and water vapor abundance. Alcohol contributions to the *m/z* 31 signal were low, on average < 4% in this home, and were accounted for in the data reduction.

VOC attribution to ions monitored by the PTR-MS was: formaldehyde *m/z* 31, methanol *m/z* 33, acetaldehyde *m/z* 45, ethanol + formic acid *m/z* 47, acrylonitrile *m/z* 54, acetone *m/z* 59, acetic acid *m/z* 61, 2-butanone *m/z* 73, benzene *m/z* 79, toluene *m/z* 93, furfural *m/z* 97, styrene *m/z* 105, C_2-alkylbenzenes + benzaldehyde *m/z* 107, hexanoic acid *m/z* 117, and monoterpenes *m/z* 137.

Natural infiltration rate calculation

The effective annual average infiltration flow rate (Q_{inf}) was calculated using a single-point envelope leakage test [11].

$$Q_{inf} = 0.052 \times Q_{50} \times wsf \times [{}^{H}/_{H_r}]^{z}$$

where Q_{inf} = estimated infiltration flow rate (cfm); Q_{50} = leakage flow rate at 50 Pa depressurization or pressurization (cfm); *wsf* = weather and shielding factor; H = vertical distance between the lowest and highest above-grade points within the pressure boundary (ft); H_r = reference height, 8.2 ft; z = 0.4. A blower door test was conducted on this house following ISO standard 9972, which determined Q_{50} as 640 cfm. The height of the vaulted ceiling in the main space (15.9 ft) was used as H. Based on the ASHRAE 62.2 (2016), *wsf* was 0.54. Given the estimated volume of the house as 27,800 ft^3 (787 m^3), the effective annual average infiltration rate was 0.05 hr^{-1}. Given the uncertainty in the Q_{50} as 4.2% and another 10% uncertainty of house volume measurement, the propagated uncertainty of the effective annual average infiltration rate is about 11% (~0.01 hr^{-1}).

Pollutant time series

Figures S-1 to S-3 illustrate indoor and outdoor mixing ratios of measured pollutants. In general indoor VOC levels were much larger than outdoors. The ion at *m/z* 117 attributed to hexanoic acid displayed a relatively invariant and arguably elevated outdoor level. We believe outdoor levels were impacted by cross contamination of the PTR-MS sampling inlet from the elevated indoor levels.

Change in VOC concentration with time when HRV was turned off

Figures S-4 and S-5 show the resulting increase in VOC concentrations when the HRV was turned off for 24 hours. The data are fit to determine the steady state concentration (*Css*) and the loss coefficient term ($n+k$) given in equation 4. Only the first 12 hours of the formaldehyde trend were fit as formaldehyde quickly reached steady state at ~ 55 ppbv. It is clear that some change in conditions occurred ~14 hours after the HRV was turned off, likely a change in infiltration rate due to a change in wind direction. At this time (~10 PM) formaldehyde concentrations slowly increased to about 62 ppbv over the next 8 hours.

Comparison of concentration time trends for ventilation off experiments

Figure S-6 shows the resulting change in VOC concentration when the HRV was turned off. The plot shows data from two different time periods when this was done to compare rates of concentration increase. The first period was for 9 hours on August 20. The second period shows the data from the 24 hour fan off period starting August 23. Concentrations and rates of change were very similar for both HRV off periods.

Change in VOC concentration with time when ventilation was turned on

Figures S-7 and S-8 show the change in VOC concentration with time when the HRV was turned back on at the high air flow rate (180 CFM) during August 21. The data are fit to determine the steady state concentration (*Css*) and the loss coefficient term ($n+k$) given in equation 4. For hexanoic acid, the change in concentration is not as fast as the other VOCs. We believe this is a consequence of the compound adsorbing to sampling inlet lines and slowly desorbing from these surfaces as the room concentrations decreased.

Formaldehyde mixing ratios and measured ACH with continuous ventilation at 180 CFM

Figure S-9 shows formaldehyde concentration, wind speed, difference in temperature between indoors and outdoors, and measured air change rate from CO_2 tracer release experiments for the time period when the ventilation was on at the high air flow rate of 180 CFM during the initial part of the study. The averaging intervals used to determine whole house emission rates of VOCs are shown. Emission rates were determined from a 3 hour average of indoor and outdoor concentrations at the end of each interval.

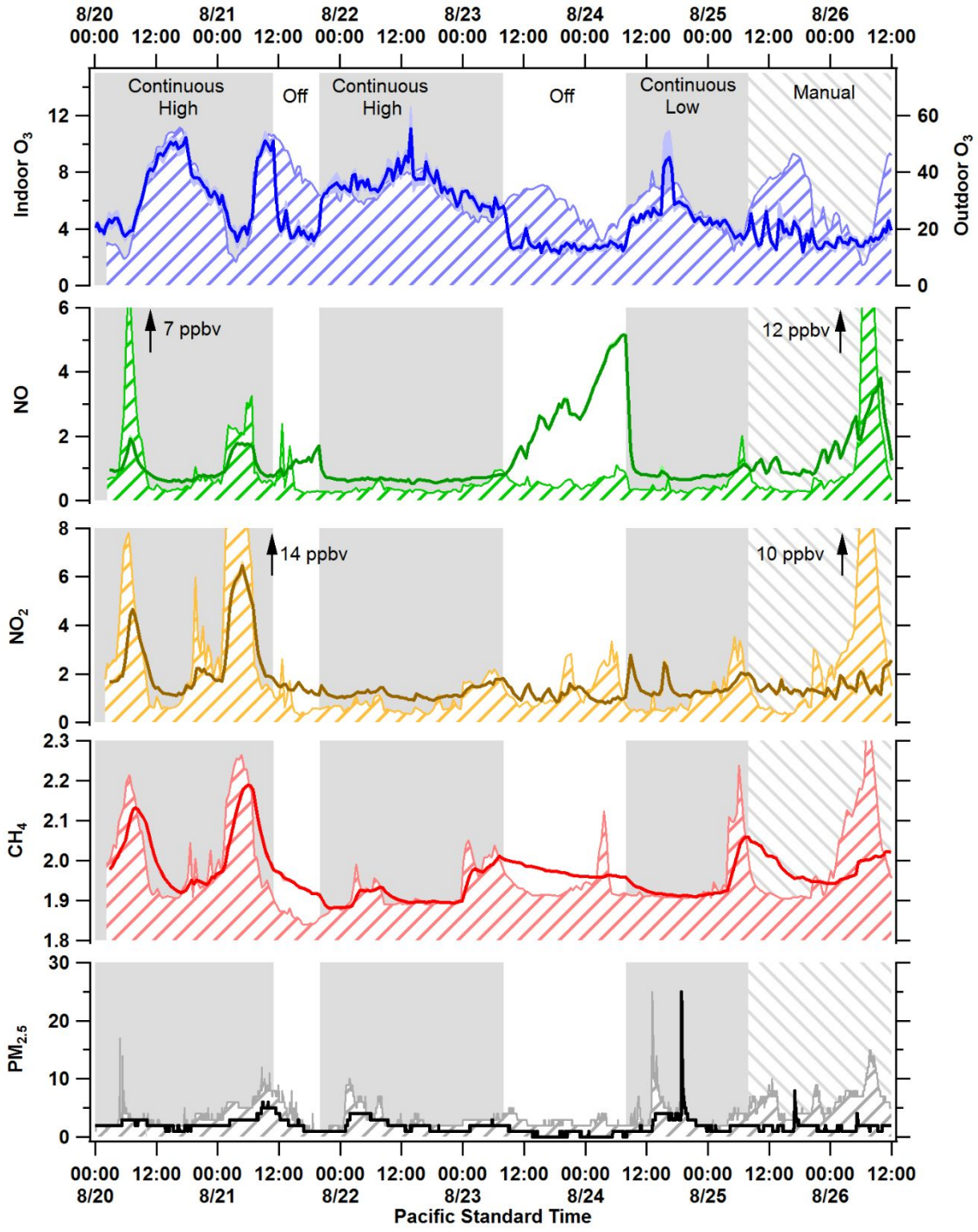

Figure S-1. Time series of O_3, NO, NO_2, and CH_4 mixing ratios (ppbv) shown as 15-min averages obtained every 30 minutes. Indoor data are displayed as solid lines (with 1-sigma standard deviation as shading) and outdoor data as filled, banded trace. Two-minute $PM_{2.5}$ concentrations (μg m^{-3}) with indoor levels are displayed as a black solid line and outdoor levels shown as a filled, banded trace. The grey background shading indicates the state of the HRV fans used to ventilate the house. Time periods when NO and NO_2 are off-scale are labeled.

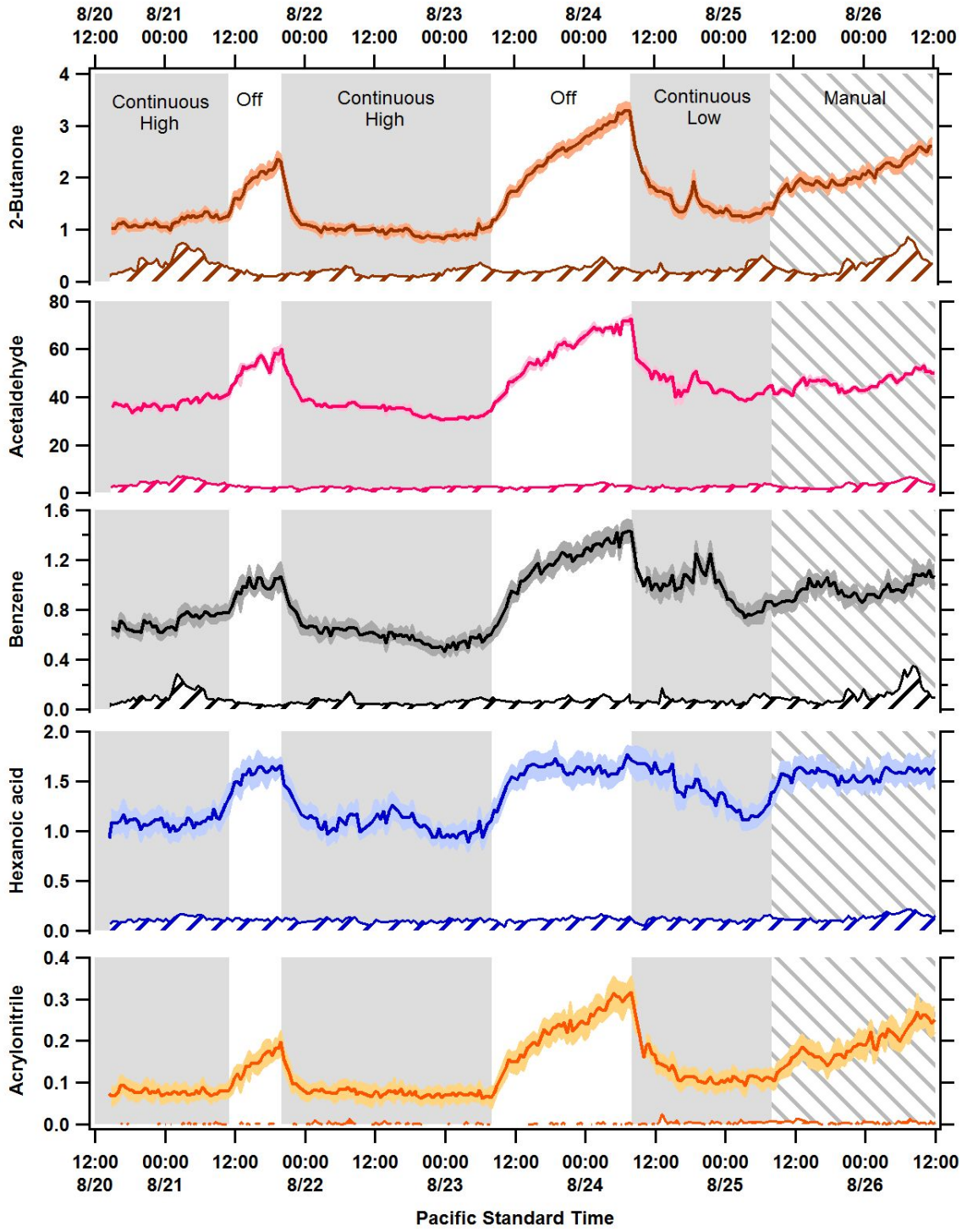

Figure S-2. Time series of VOC mixing ratios (ppbv). The data are 15-min averages obtained every 30 minutes. Indoor data are displayed as solid lines (with 1-sigma standard deviation as shading) and outdoor data as filled, banded trace. The grey background shading indicates the state of the HRV fans used to ventilate the house.

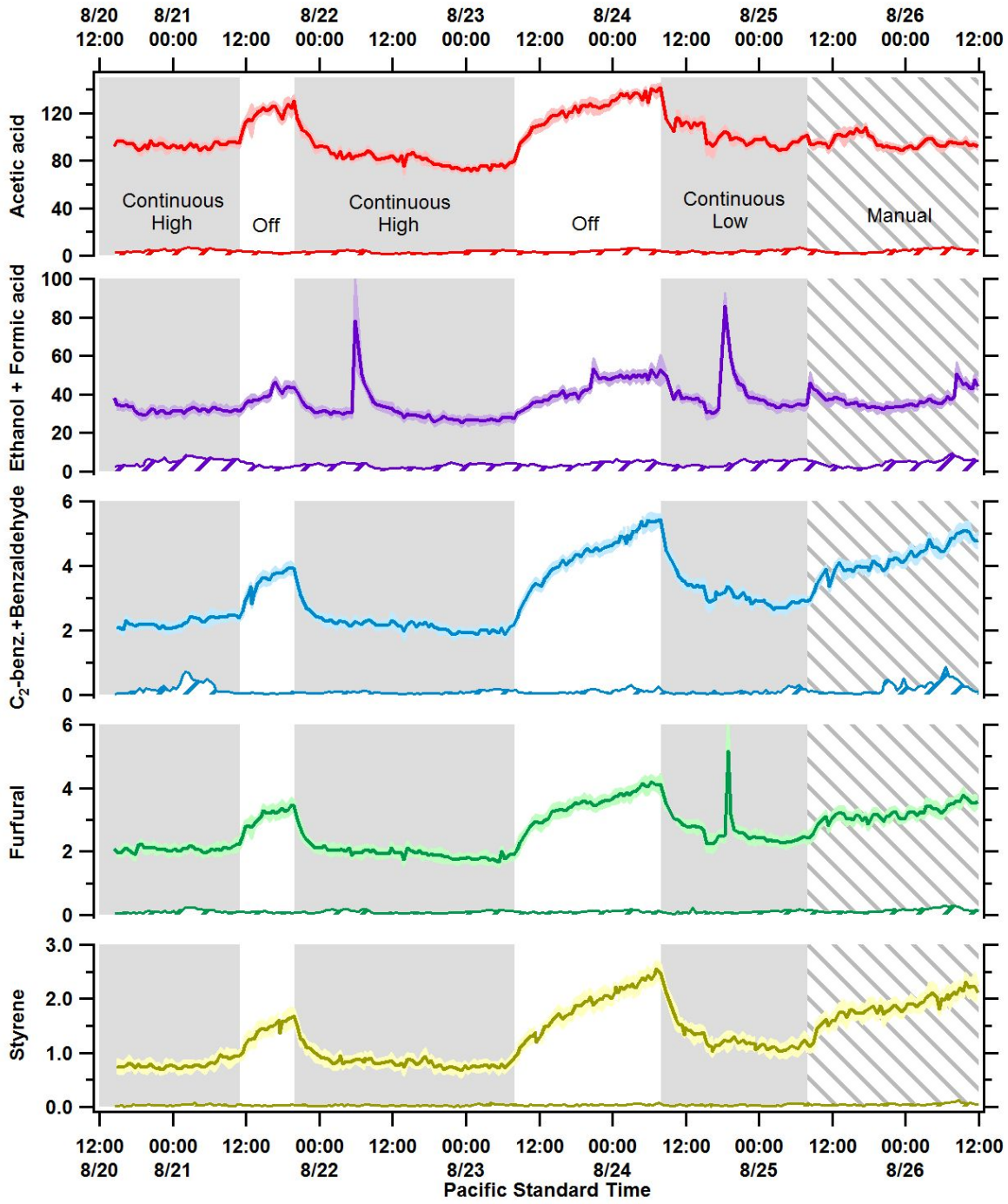

Figure S-3. Time series of acetic acid and other four VOCs in ppbv. The data are 15-min averages obtained every 30 minutes. Data for indoor are displayed as solid lines (with 1-sigma standard deviation as shading) and outdoor data as filled, banded trace. The grey background shading indicates the state of the HRV fans used to ventilate the house.

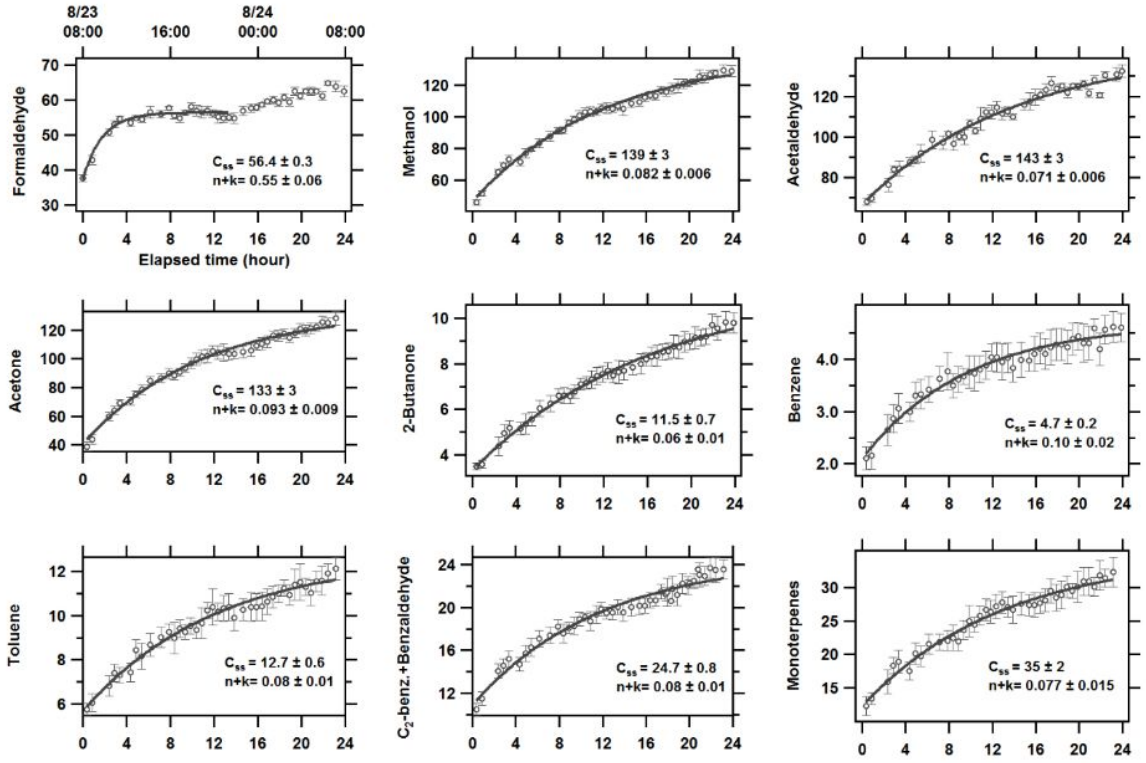

Figure S-4. Change in VOC concentration (μg m^{-3}) with time in when the HRV fan was turned off from 8 am PST on Aug 23rd to 8 am PST on Aug 24th. Shown are 15-minute averages with 1-sigma standard deviations shown as error bars. Data are fitted with Eq. 4 shown as the solid line to determine steady-state concentration C_{ss} in μg m^{-3} and the term $n+k$ in hr^{-1}.

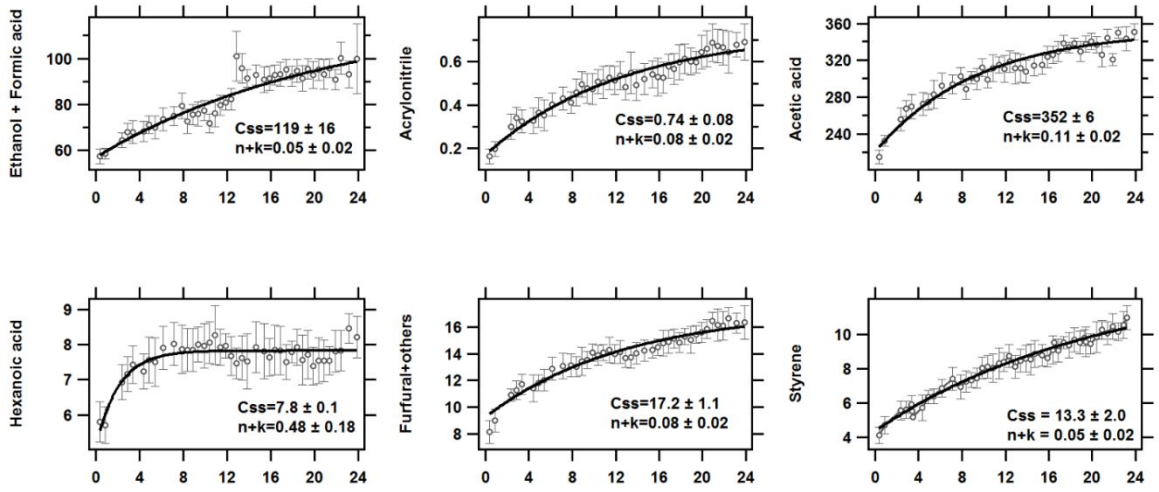

Figure S-5. Change in VOC concentration (μg m^{-3}) with time in when the HRV fan was turned off from 8 am PST on Aug 23rd to 8 am PST on Aug 24th. Shown are 15-minute averages with 1-sigma standard deviations shown as error bars. Data are fitted with Eq. 4 shown as the solid line to determine steady-state concentration C_{ss} in μg m^{-3} and the term $n+k$ in hr^{-1}.

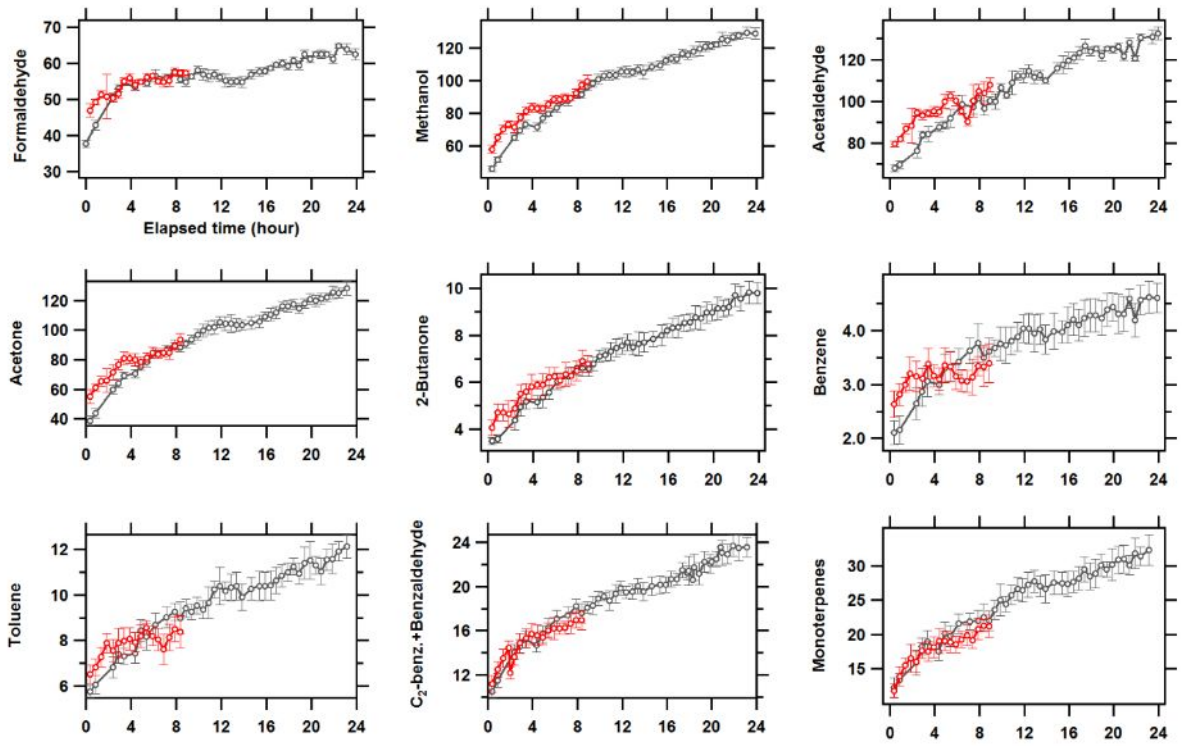

Figure S-6. Time series of increases in concentration (μg m^{-3}) during the first (red symbols) HRV fan-off experiment (11 am PST - 8 pm PST on Aug. 20th,) and the second (black symbols) HRV fan-off experiment (8 am PST on Aug. 23rd - 8 am PST on Aug. 24th). Shown are 15-minute averages with 1-sigma standard deviations as error bars.

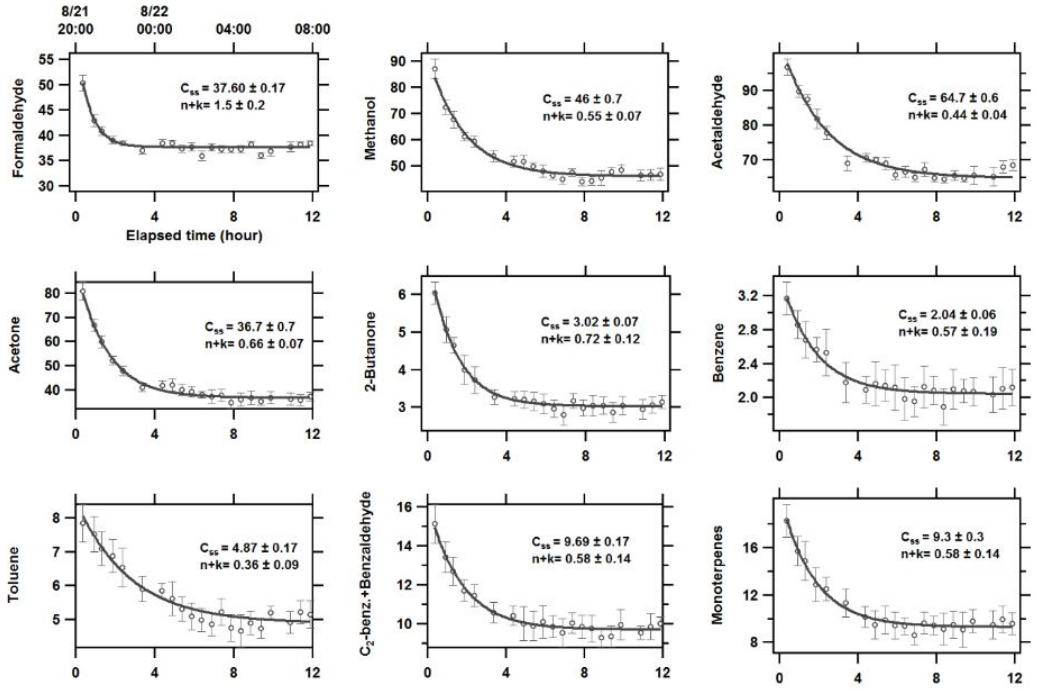

Figure S-7. Change in VOC concentration (μg m^{-3}) with time in when the HRV fan was turned back on (from 8 pm PST on Aug 21st to 8 am PST on Aug 22nd). Shown are 15-minute averages with 1-sigma standard deviations shown as error bars. Data are fitted with Eq. 4 shown as the solid line to determine steady-state concentration C_{ss} in μg m^{-3} and the term $n+k$ in hr^{-1}.

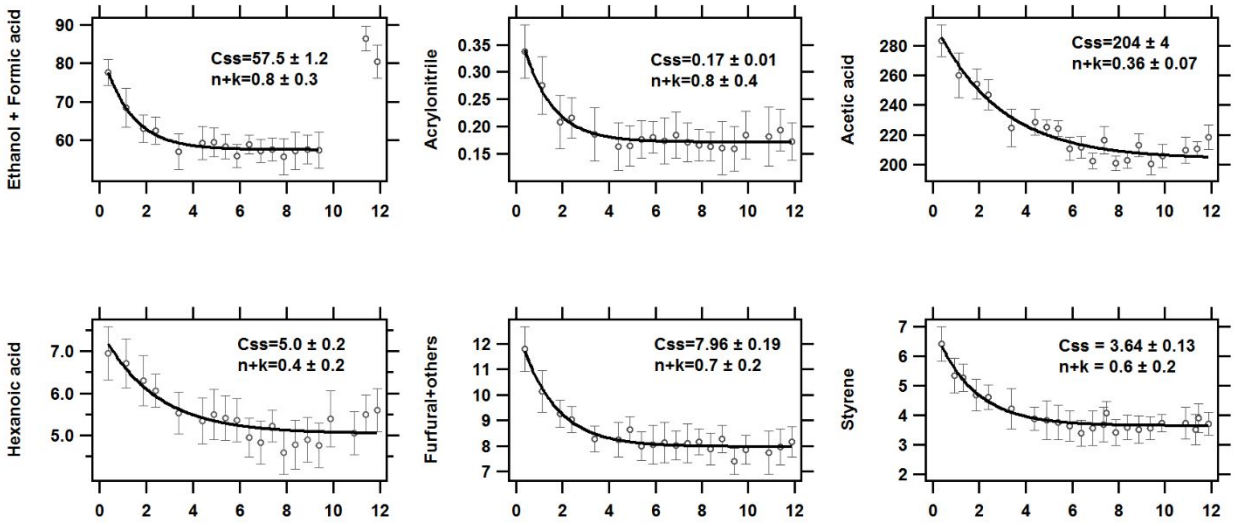

Figure S-8. Change in VOC concentration (μg m^{-3}) with time in when the HRV fan was turned back on (from 8 pm PST on Aug 21st to 8 am PST on Aug 22nd). Shown are 15-minute averages with 1-sigma standard deviations shown as error bars. Data are fitted with Eq. 4 shown as the solid line to determine steady-state concentration C_{ss} in μg m^{-3} and the term $n+k$ in hr^{-1}.

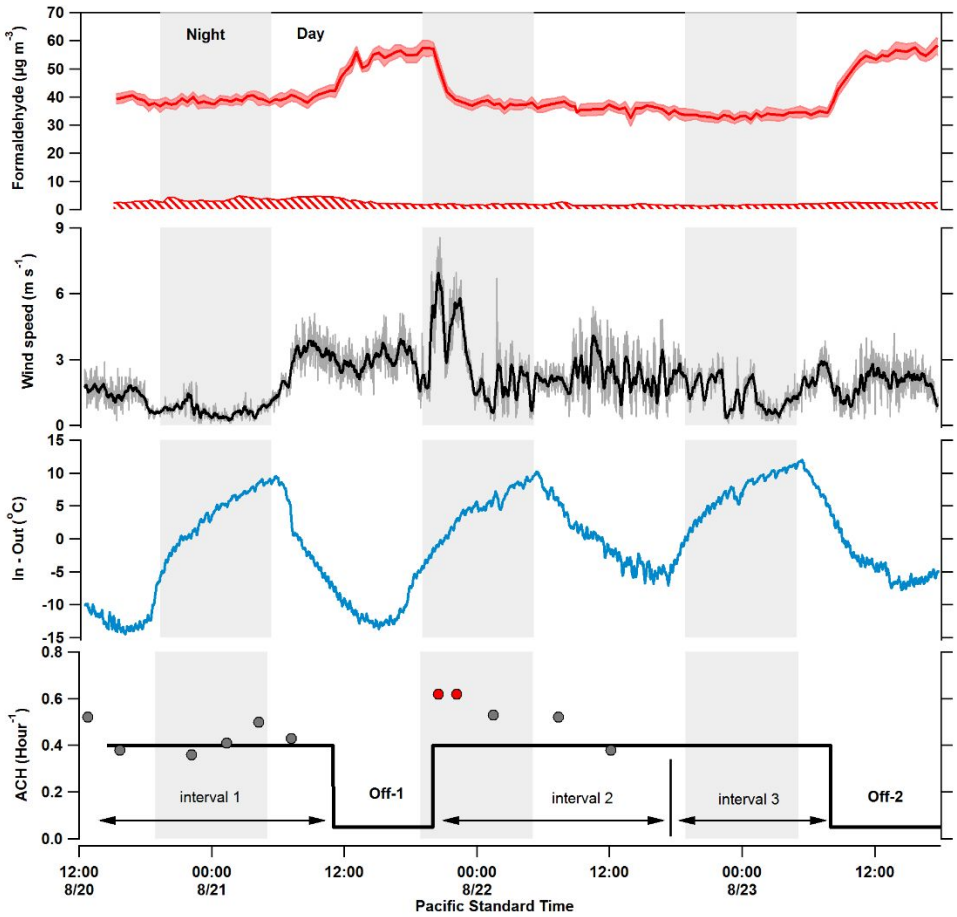

Figure S-9. Indoor (solid trace) and outdoor (banded trace) formaldehyde concentrations, wind speed, indoor outdoor temperature difference and measured air change rates for the period when the HRV was operated at high air flow. Wind speeds at 10-m (grey) with 20-minute smoothing (black trace) are shown. Bottom panel displays the expected ACH of 0.40 hr^{-1} (black solid line) with the HRV on and when it was turned off (estimated as 0.05 hr^{-1}). Measured ACH are shown as circles. Two measured ACH data points are highlighted with red color to show the impact of elevated wind speed during that time period. Daytime and nighttime periods are shown by shading. Intervals for calculating emission rates are shown.

Table S-1. Ventilation on data listing average steady-state concentrations (C_{ss}, μg m^{-3}), outdoor concentration (C_a, μg m^{-3}), whole house emission rates (S, mg hr^{-1}), and area specific emission rates (E, μg m^{-2} hr^{-1}).

m/z	VOC	C_{ss}	C_a	S	E
61	Acetic acid	207 ± 2	10.9 ± 0.4	68 ± 9	227 ± 31
45	Acetaldehyde	65.7 ± 0.4	5.8 ± 0.1	21 ± 3	70 ± 10
33	Methanol	46.1 ± 0.5	6.8 ± 0.2	14 ± 2	46 ± 7
59	Acetone	36.9 ± 0.6	6.7 ± 0.3	11 ± 2	35 ± 6
47	Ethanol + formic acid	55.8 ± 0.9	9.3 ± 0.5	16 ± 2	54 ± 8
31	Formaldehyde	37.1 ± 0.2	2.79 ± 0.06	26 ± 2*	86 ± 8
137	Monoterpenes	9.8 ± 0.2	0.64 ± 0.08	3.2 ± 0.4	11 ± 2
107	C2-alkylbenzene+ Benzaldehyde	9.6 ± 0.1	0.50 ± 0.04	4.1 ± 0.5	14 ± 2
97	Furfural + others	7.7 ± 0.2	0.52 ± 0.05	2.5 ± 0.3	8.3 ± 1.2
105	Styrene	3.3 ± 0.1	0.18 ± 0.03	1.1 ± 0.2	3.7 ± 0.5
93	Toluene	5.11 ± 0.08	0.50 ± 0.03	1.6 ± 0.2	5.4 ± 0.8
73	2-Butanone	3.12 ± 0.06	0.85 ± 0.03	0.8 ± 0.1	2.6 ± 0.5
79	Benzene	2.09 ± 0.05	0.31 ± 0.02	0.6 ± 0.1	2.1 ± 0.3
117	Hexanoic acid	4.92 ± 0.12	0.55 ± 0.06	3.1 ± 0.5*	10.3 ± 1.6
54	Acrylonitrile	0.16 ± 0.01	< DL **	0.06 ± 0.01	0.19 ± 0.03

*Decay coefficient was applied. 0.47 hr^{-1} for formaldehyde and 0.40 hr^{-1} for hexanoic acid.
**Below detection limit.

The importance of including the decay coefficient in the emission rate calculation: case evaluation

In the steady-state emission rate calculation (Eq. 3 in the manuscript), the decay coefficient is as important as air change rate. Only a few papers reported the air change rate used in the formaldehyde whole house emission rate calculation, where the impact of including the decay coefficient in the emission rate calculation can be evaluated by assuming no outdoor contribution. Two cases are discussed below.

Poppendieck et al.[4] studied a net-zero energy house focusing on the evaluation of using low VOCs emission materials in the house. The net-zero energy house was a two-story, detached home with permanently installed cabinetry, other than the cabinetry no other wood material such as furniture, was placed inside the house. The materials used to construct the house were selected with care to be low VOC emission materials. Emission rates were measured one year and two years after the house was built. With indoor temperature measured as 23 ^{o}C, averaged formaldehyde emission rates in both phases were 6.7 μg m^{-2} hr^{-1}, a factor of 12 lower than 82 μg m^{-2} hr^{-1} measured in our study with the ventilation turned off. The source control approaches by using low emission materials greatly reduced the whole house emission factors, however, this paper omitted the loss of formaldehyde in the emission factors calculation. Given the ACH stated in the paper (0.18 hr^{-1} as the average of two phases) and applying 0.47 hr^{-1} decay coefficient from our study, the emission factors of formaldehyde is revised upward to be 24.2 μg m^{-2} hr^{-1}; omitting the loss of formaldehyde causes a severe underestimation. Since this house was not furnished, the loss and the source of formaldehyde may not be directly comparable to our results.

Offermann et al. [13,14] studied 108 new single-family, detached homes in CA, during which the levels of 22 VOCs were measured as well as the ACH. All the houses measured were

occupied and furnished, with house ages ranging from 1.7 years to 5.5 years. Indoor volume-specific emission rates for formaldehyde, acetaldehyde, and benzene were presented which can be converted to emission factors by assuming the 2.6-meter ceiling height. With the loss term omitted, the median emission factor of formaldehyde was 29 μg m^{-2} hr^{-1}, much lower than our results. Based on the ACH and emission factor data stated for Home 033 in that report, the formaldehyde emission factors in μg m^{-2} hr^{-1} can be corrected and are displayed in Table S-2. It was found that the formaldehyde emission factors may be underestimated by up to 78% and the corrected emission rate (98 μg m^{-2} hr^{-1} by average) is comparable with our results (81 μg m^{-2} hr^{-1} and 86 μg m^{-2} hr^{-1} at different ACH). In addition, the original data showed that as ACH increased from 0.13 hr^{-1} to 0.29 hr^{-1}, formaldehyde emission factors also increased from 20.8 μg m^{-2} hr^{-1} to 36.4 μg m^{-2} hr^{-1}. After the correction for indoor loss, the formaldehyde emission rates lose their ACH dependency. From Offermann et al. [13], the indoor temperatures during the measurements varied from 17 ^{o}C to 28 ^{o}C with the median as 22 ^{o}C, but no particular indoor temperature was reported for Home 033 so variation in formaldehyde emission rates may be due to both ACH and temperature change.

Table S-2. Formaldehyde emission rate adjustment based Home 033 data in Offermann et al.'s report [13]. Emission rates are shown in μg m^{-2} hr^{-1}.

ACH (hr^{-1})	Reported Emission rate	Corrected Emission factor
0.13	20.8	96
0.23	33.8	103
0.29	36.4	95

*Assuming 0.47 hr^{-1} decay coefficient and omitting outdoor contribution.

References:

1. Su., T and W.J. Chesnavich, Parameterization of the ion-polar molcule collision rate constant by rajectory calculations, *J. Chem Phys*., 76, 5183-5185, 1982.

2. Su., T., Erratum: Trajectory calculations on ion-polar molecule capture rate constants at low temperatures, *J. Phys. Chem*., 89, 5355, 1988.

3. Jobson, B.T., J.K. McCoskey, Sample drying to improve HCHO measurements by PTR-MS instruments: Laboratory and field measurements, *Atmos. Chem. Phys*. 10 (2010) 1821–1835. doi:10.5194/acp-10-1821-2010.

4. Karl, T., Use of proton-transfer-reaction mass spectrometry to characterize volatile organic compound sources at the La Porte super site during the Texas Air Quality Study 2000, *J. Geophys. Res.* 108 (2003) 4508. doi:10.1029/2002JD003333.

5. Karl, T.G., T.J. Christian, R.J. Yokelson, P. Artaxo, W.M. Hao, A. Guenther, The tropical forest and fire emissions experiment: Method evaluation of volatile organic compound emissions measured by PTR-MS, FTIR, and GC from tropical biomass burning, *Atmos. Chem. Phys*. 7 (2007) 5883–5897. doi:10.5194/acp-7-5883-2007.

6. Vlasenko, A. A.M. MacDonald, S.J. Sjostedt, J.P.D. Abbatt, Formaldehyde measurements by Proton transfer reaction - Mass spectrometry (PTR-MS): Correction for humidity effects, *Atmos. Meas. Tech*. 3 (2010) 1055–1062. doi:10.5194/amt-3-1055-2010.

7. Spanel, P., D. Smith, SIFT studies of the reactions of H_3O+, NO+ and O_2+ with a series of alcohols, *Int. J. Mass Spectrom. Ion Process*. 167–168 (1997) 375–388. doi:https://doi.org/10.1016/S0168-1176(97)00085-2.

8. Spanel, P., D. Smith, Quantification of trace levels of the potential cancer biomarkers formaldehyde, acetaldehyde and propanol in breath by SIFT-MS, *J. Breath Res*. 2 (2008) 046003. doi:10.1088/1752-7155/2/4/046003.

9. Inomata, S., H. Tanimoto, S. Kameyama, U. Tsunogai, H. Irie, Y. Kanaya, Z. Wang, Technical Note: Determination of formaldehyde mixing ratios in air with PTR-MS: laboratory experiments and field measurements, *Atmos. Chem. Phys*. 8 (2008) 273–284. doi:10.5194/acp-8-273-2008.

10. Schripp, T., C. Fauck, T. Salthammer, Interferences in the determination of formaldehyde via PTR-MS: What do we learn from *m/z* 31?, *Int. J. Mass Spectrom*. 289 (2010) 170–172. doi:10.1016/j.ijms.2009.11.001.

11. ASHRAE, *ANSI/ASHRAE Standard 62.2-2016. Ventilation and Acceptable Indoor Air Quality in Residential Buildings*. (2016). American Society for Heating, Refrigeration, and Air Conditioning Engineers, Inc.: Atlanta, GA.

12. Poppendieck DG, Ng LC, Persily AK, Hodgson AT. Long term air quality monitoring in a net-zero energy residence designed with low emitting interior products. *Build Environ*. 2015;94:33–42. 2015. http://dx.doi.org/10.1016/j.buildenv.2015.07.001.

13. Offermann FJ. *California Energy Commission Ventilation and Indoor Air Quality in New Homes*.; 2009. https://www.arb.ca.gov/research/apr/past/04-310.pdf.

14. Offermann FJ, Hodgson AT. Emission rates of volatile organic compounds in new homes. *12th International Conference on Indoor Air Quality and Climate 2011*. http://www.scopus.com/inward/record.url?eid=2-s2.0-84880558115&partnerID=tZOtx3y1. Accessed August 24, 2018.